

Inorganic scintillator surface enhancements with 2-D photonic crystals to improve light collection

Stuti Surani^{1,*}, Faruk Logoglu¹, Patrick Albert², Dr. Douglas Wolfe², and Dr. Marek Flaska¹

¹Ken and Mary Alice Lindquist Department of Nuclear Engineering

²Department of Materials Science and Engineering

Pennsylvania State University, United States of America

(*) srs6376@psu.edu

Abstract— Inorganic scintillators are widely used in various applications of gamma spectroscopy such as nuclear nonproliferation and safeguards, medical applications, space applications, and astronomy. This is due to good energy resolution, stable performance, somewhat low cost, and relatively high detection efficiency. However, many inorganic scintillators have high refractive indices and suffer significant light losses due to total internal reflection (TIR). This project proposes using optimized periodic nanostructures called photonic crystals to recover some of the light originally lost due to TIR. Photonic crystals provide an optical bridge (constructive interference) between the scintillator and the photosensor for the trapped light photons. Improving the light extraction can improve the energy and time resolutions of the scintillator, allowing for a wider range of research and industry applications. Photonic crystals can be optimized in terms of their dimensions, shapes, and materials to maximize the light extraction. Preliminary optimization tests were performed using a LYSO scintillator coupled with Si₃N₄ photonic crystals. First, a realistic light input source is obtained by simulating the scintillation process in Monte Carlo code Geant4. The simulated scintillation photons are collected at the LYSO-PMT boundary to obtain their energy and angular distributions. In the next step, a deterministic code OptiFDTD is used to simulate light interactions with different nanostructures. Currently, the simulations are limited to 2-D block nanostructures. The optimization tests vary the height, width, and spacing of the photonic crystals. Preliminary optimization tests show an improvement in the light transmission by more than 60%. The optimized geometry will be manufactured in the lab using various manufacturing techniques such as ion milling, electron beam lithography, or 3D printing. Various gamma sources will be used to experimentally characterize the LYSO scintillators with and without photonic crystals. These experiments will also be used to validate the simulations and demonstrate the effectiveness of the photonic crystals in improving the energy resolution. Once validated, the simulations will be used to determine optimized photonic crystals for other inorganic scintillators, such as bismuth germanate, sodium iodide, and lanthanum bromide.

Keywords — Photonic crystals, nanostructures, light output, inorganic scintillators

I. INTRODUCTION

Inorganic scintillators are essential for various applications, including nuclear security, medical applications such as PET, high energy physics, and industrial control [1]. In recent years, scintillator development has been focused on improvements in energy resolution for homeland security applications and time resolution for medical applications. Inorganic scintillators are more versatile than semiconductors but typically lack the high energy resolution of semiconductors. A scintillator's energy and time resolution can be improved by improving the light output [2]. While most inorganic scintillators have a high light yield, the light output is lower due to various light loss mechanisms at play, such as absorption within the crystal, crystal defects, refraction through the remaining sides of the crystal, and most importantly, total internal reflection (TIR) at the scintillator photosensor interface.

Photonic crystals (PHCs) are nanostructures theorized to improve light output by reducing light loss due to TIR. PHCs have been used for various light applications, such as LEDs, optical fibers, and solar cells [3,4]. These nanostructures of high refractive index material act as periodic alternating dielectric media at the crystal surface. PHCs, thus, provide an optical bridge for photons of a specific wavelength through interference and diffraction [2,3]. The nanostructure pattern for the PHCs must be optimized for the light emission spectrum of the given scintillator. To do this, we must simulate both the scintillation process within the scintillator and the light modes produced by the PHCs at the scintillator-photosensor interface.

Manufacturing such nanostructures can be expensive and time-consuming depending on the required spatial resolution of the resulting nanostructures. We have chosen a LYSO scintillator and a BGO scintillator for our initial tests. LYSO was chosen for its prevalence in literature for PHC development [5,6]. The scintillators are coupled with a pillar array geometry, using silicon nitride (Si₃N₄) as the PHC material due to its inherently high refractive index. Once manufactured, the scintillators will be characterized with a gamma source to note relative improvements in light output and energy resolution. This paper will discuss the simulation and optimization of PHCs, the manufacturing techniques, and preliminary efforts to characterize the scintillators with a gamma source.

II. METHODOLOGY

The project is broadly divided into four parts: macroscale light transport simulations in Geant4 [7], PHC optimization simulations in OptiFDTD [8], manufacturing the optimized PHC geometry using electron beam lithography, and characterization of scintillators by radiation measurements with a gamma source, as shown in the flowchart in Fig. 1.

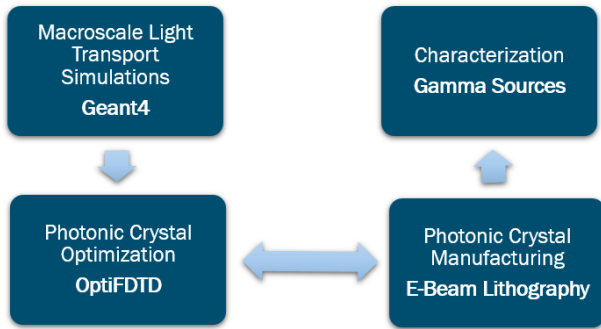


Fig. 1. Flowchart for the project.

The simulations consist of macroscale light transport and nanoscale light transport, a division required to fully simulate the light transport through the scintillator and the effects at the nanoscale level with the PHCs. The next step is manufacturing the optimized PHC geometry and characterizing it using a gamma source.

The radiation measurements provide us with validation for the simulation model, along with helping identify issues with the fabrication process. All the steps are interlinked as the simulations provide the manufacturing template, and the radiation measurements and manufacturing provide data to make the simulations more realistic and account for the manufacturing constraints.

We use a LYSO and a BGO scintillator for our initial tests coupled to a block structure Si_3N_4 PHC. The material data for LYSO and BGO is given below in Table. I.

TABLE I
MATERIAL DATA FOR SCINTILLATORS

Properties	LYSO	BGO
Dimensions	10 mm × 10 mm × 3 mm	10 mm × 10 mm × 2.5 mm
Refractive Index	1.81	2.15
Light Output (Photons/keV)	33	9
Decay Time (ns)	36	300

The two scintillators have similar dimensions and emission spectra. Thus, we expect similar energy and angular distribution of light at the scintillator photosensor boundary. BGO has a higher refractive index than LYSO, so it has a higher percentage of internally reflected photons. We thus expect to observe a more significant improvement in BGO transmission than LYSO transmission for the optimized PHC geometry.

A. Simulations

PHCs provide an optical bridge for light photons of a specific wavelength to escape the scintillator and reach the photosensor. However, the PHC geometry must be optimized for the scintillator material and geometry. Simulating light transport through the PHCs allows us to optimize the PHC geometry for a given material.

We first simulated the macroscale light transport within the scintillator using a Monte Carlo code called Geant4. Geant4 simulates the scintillation process and light transport in the scintillator, as shown in Fig. 2. A point gamma source simulates the Cs-137 source used for the radiation measurement process. Each gamma interaction within the scintillator yields an isotropic production of optical photons within the scintillator consistent with the emission spectrum of the scintillators. These photons are then transported as particles through the scintillator material, and they undergo absorption, reflection, refraction, and scattering in the material. The photon's energy and angular distribution is then tallied at the scintillator-photosensor interface. These energy-angle maps produce the light input source for the nanoscale simulations [9]. The material data for these simulations is obtained from UV-vis measurements.

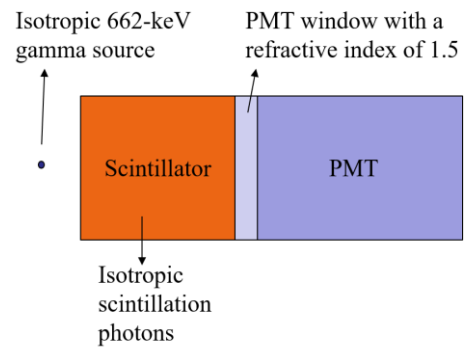


Fig. 2. Geant4 simulation geometry for macroscale light transport within the scintillator.

The nanoscale simulations are done in OptiFDTD, a deterministic code that models light as electromagnetic waves, thus allowing for a more complex treatment of light transport through the PHCs. The input source for OptiFDTD is obtained from the Geant4 simulations. At this point, the source only consists of the first pass of light through the scintillator-photosensor interface. The light reflected from the sides of the scintillator is not accounted for. Future simulations will include multiple reflections, making the simulations more realistic and allowing for more light transmission.

The optimization simulations are done as shown in Fig. 3. For these initial tests, a 2D block structure geometry is selected for the PHCs. The input source obtained from Geant4 is modeled as a planewave within the scintillator. It then interacts with the PHCs and is detected within the PMT, modeled as a dielectric material with a refractive index of 1.5. The material data for these simulations are obtained from ellipsometry measurements. There are three variables of interest:

- The height of the PHC (PHC z)
- The thickness of the PHC (PHC x)
- The spacing between the PHC (Gap)

The simulations vary these variables from 0.1 μm to 1 μm for ten iterations each. The results are then tallied as a function of the percentage of light transmission to the PMT. The spacing between the PHC can be modeled as a vacuum to simulate a dry coupling or as optical grease to simulate a grease coupling. For our initial tests, we only model dry coupling.

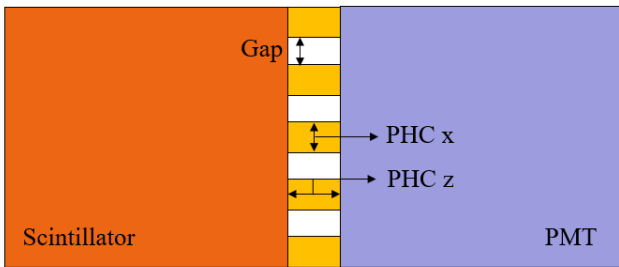


Fig. 3. OptiFDTD simulation geometry for nanoscale light transport and PHC optimization.

B. Manufacturing

For this effort, the manufacturing of PHCs is carried out using various techniques broadly divided into either top-down or bottom-up approaches, as shown in Fig. 4. Bottom-up processes include self-assembly of polystyrene nanospheres via spin casting. This method is both scalable and inexpensive. Top-down approaches explored include ion milling, laser write methodologies, and electron beam lithography. Each approach has its associated advantages and disadvantages. The top-down processes can have the advantage of extremely high pattern resolution, which allows for greater control over manufacturing the pattern of interest. Electron beam lithography, while marginally more expensive than the bottom-up processes and the other aforementioned top-down approaches, offers the ability to pattern nanoscale features with high spatial resolution.

Furthermore, it is an industry-available technology that can be scaled up for manufacturing if required. Our initial tests focus on electron beam lithography and dry etching to replicate the modeled geometry and verify the simulations. However, future work will focus on 3D simulations of nanospheres to explore the economic feasibility for different applications.

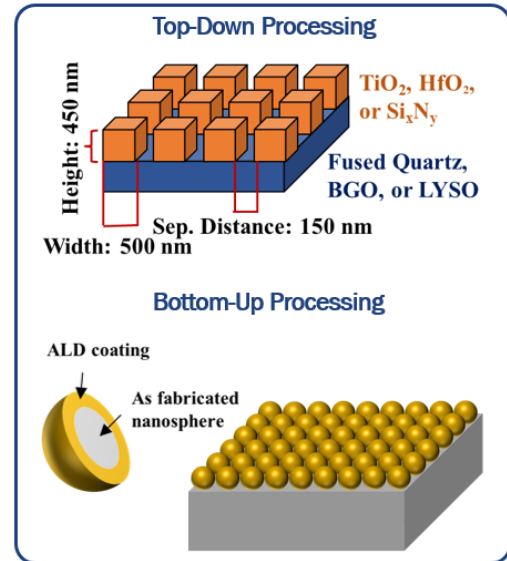


Fig. 4. Manufacturing approaches for PHCs.

PHCs can be made from any dielectric material with a high refractive index as compared to the refractive index of the base scintillator—some favorable materials for this type of processing are TiO_2 , HfO_2 , and Si_3N_4 . For LYSO, we chose Si_3N_4 for its refractive index of approximately 2.01 at 415 nm, relative to the refractive index of LYSO (1.83). The complete PHC manufacturing methodology is explained in the flowchart in Fig. 5. First, we identify our substrate, which is the LYSO scintillator material. We then perform radiation baseline measurements to provide a reference light yield and energy resolution. After cleaning the crystals, we deposit a thin (300 nm) Si_3N_4 film onto the scintillator using radio frequency (RF) reactive sputtering at room temperature. The PHC geometry, or pattern, is then transferred onto this thin film through electron beam lithography. The first step is to deposit a resist layer, or polymer-based film, using spin casting onto the surface of the silicon nitride. Next, a thin gold layer is deposited to aid in conductivity during the electron beam writing process to help mitigate charge build-up. Finally, we can use an electron beam lithography tool to write the pattern, or PHC geometry, into the photoresist to cure. The sample is then transferred into a reactive ion etch chamber to mill or etch away the silicon nitride, leaving behind the pillar geometry. The gold and photoresist layers are then removed to reveal the pattern on the substrate of our finished PHC.

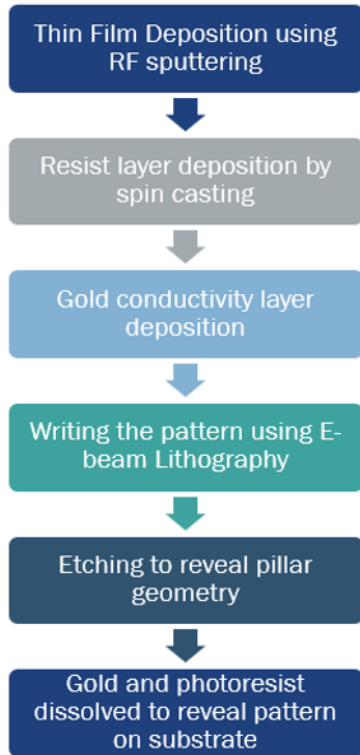


Fig. 5. Flowchart for manufacturing PHCs using dry etching and electron beam lithography.

C. Radiation Measurements

The radiation measurements for the scintillators are done using a Cs-137 gamma source. The experimental geometry is shown in Fig. 6. The scintillator is placed on a Hamamatsu H10580 PMT and kept stable using a 3D-printed PMT holder. The PMT is connected to a CAEN DT5730 digitizer which processes the analog signals from the PMT and converts them to digital signals processed by a computer software called CoMPASS, also provided by CAEN. The PMT is also connected to a high-voltage power supply set to -1200 volts.

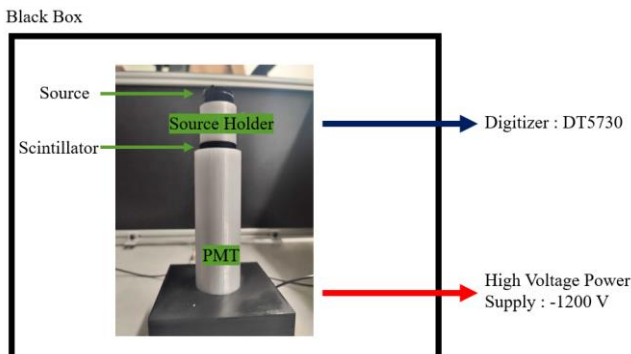


Fig. 6. Radiation measurements setup.

The source is placed on the scintillator in a 3D-printed source holder. The source consists of four ^{5u}Ci Cs-137 sources stacked on each other and taped together, as given in Fig. 7. This creates

a stronger source to reduce the signal-to-noise ratio and improve the statistics. The scintillator responses are measured with and without optical grease. Measurement is done for peak counts greater than 100000 to reduce the uncertainty to less than 0.1%.



Fig. 7. Radiation source for the measurements.

Baselines measurements for bare LYSO crystals have been done with an average energy resolution of 13.3% for crystals without optical grease, and 10 % for crystals with optical grease. These measurements were done without using any reflectors to improve energy resolution. Future radiation measurements will be compared to these data to note improvements in light output and energy resolution.

Furthermore, radiation baseline measurements were done after some of the manufacturing steps to ensure that the crystal's optical properties are consistent with expected optical degradation, and to aid in influencing the optimal manufacturing flow path.

For example, one of the first manufacturing steps for PHCs is to deposit a Si₃N₄ thin film onto the scintillator (LYSO). Before formalizing the manufacturing in section B, the thin films were deposited via direct current (DC) reactive magnetron sputtering at 200°C with an applied substrate bias. At this stage, we performed radiation measurements to compare the crystal's optical properties before and after thin film deposition. The radiation measurements showed a significant decline in the light output of the scintillator. While a decrease in performance was expected, some optical effects were also observed on visual inspection, as shown in Fig. 8. These optical effects can result from coating overspray leading to thickness gradients along the edges, or the temperature and substrate bias could damage the crystal.

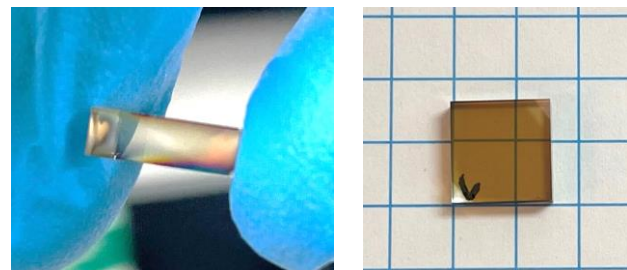


Fig. 8. Left: Thin film deposition via DC magnetron sputtering. Right: Thin film deposition via RF sputtering.

To resolve this, we investigated the optical effects when using RF sputtering for thin films. RF Sputtering, like DC sputtering, is done under a high vacuum, creating high-density, low-defect optical films. However, RF sputtering tends to have a slower deposition rate, allowing us to mitigate further defects,

and we were able to establish equivalent optical properties without needing to deposit at 200°C and substrate bias. We tested various baseline deposition conditions to study the sputtering process as a function of power, nitrogen flow, and time as shown in Fig. 9.

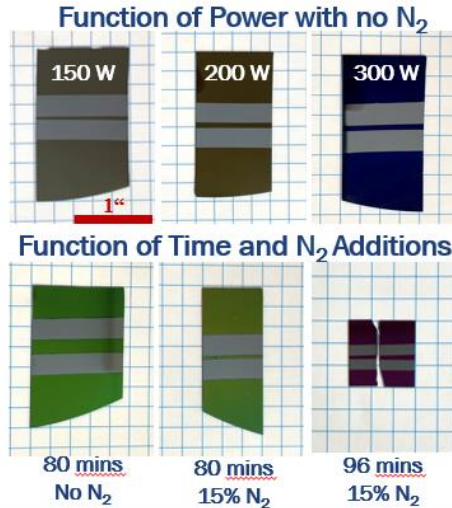


Fig. 9. Left: Thin film deposition via RF sputtering as a function of power, time, and nitrogen flow to investigate optimal processing conditions.

We found the optimal conditions to be 300 W power, 15% nitrogen flow, and a 3.125 nm/min deposition rate for our Si₃N₄ thin film. Scanning electron microscopy and ellipsometry were used to look for microstructure changes and to observe the coating thickness and refractive index. By performing radiation measurements after the thin film deposition, we identified issues with our initial process and corrected them before those effects were categorized in the final assessment of the PHC structure.

III. RESULTS

A. Optimization Simulations

The Geant4 simulations were used to produce energy-angle maps for LYSO and BGO. These data were then used to create the input source for the OptiFDTD simulations [9].

The optimization simulation results are given in Fig. 10 for a BGO scintillator and in Fig. 11 for a LYSO scintillator. The results are also summarized in Table. II.

As discussed in the methodology section, LYSO and BGO have comparable geometry and emission spectra. Thus, they both have similar optimized PHC geometry. The BGO has a higher refractive index than LYSO, resulting in a more significant improvement in light transmission with the PHCs. For LYSO, the optimized PHC geometry yields an improvement in light transmission of 46.8 %, while for BGO, the improvement is 91.9 %. For LYSO, further simulations were done with finer optimization steps to obtain a light transmission of 59%, which is an improvement of 62.8%. Improvement is calculated as relative change between the initial and final light transmission in percentage.

The simulation results are consistent with our initial expectations and show that light output improvement due to PHCs is better for higher refractive index materials.

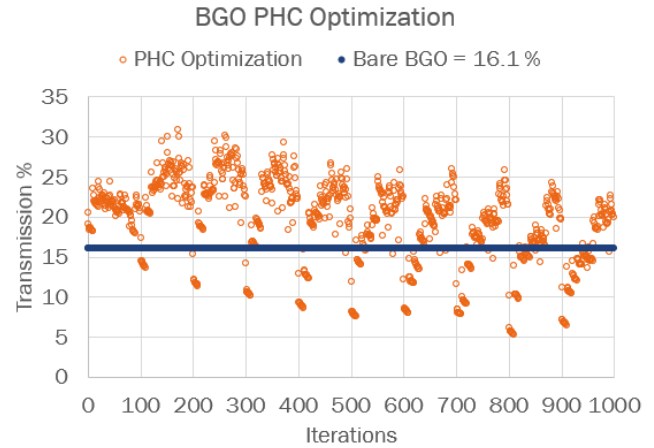


Fig. 10. Optimization simulation results for a BGO scintillator.

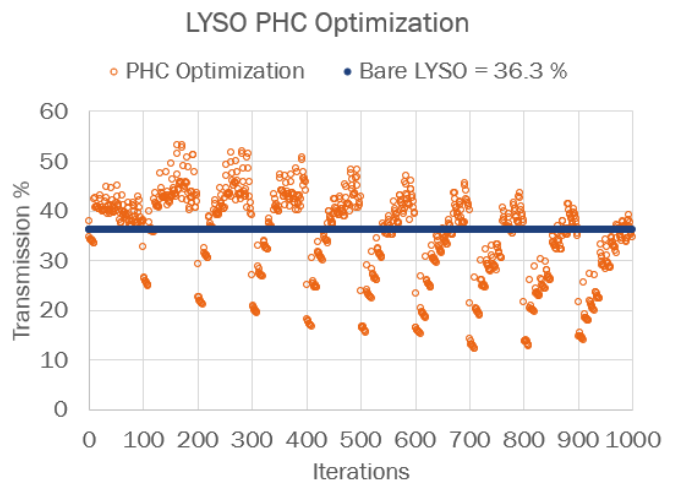


Fig. 11. Optimization simulation results for a LYSO scintillator.

TABLE II
 OPTIMIZATION RESULTS FOR LYSO AND BGO

Material	Initial Transmission	Gap (μm)	PHC x (μm)	PHC z (μm)	Final Transmission	Improvement
LYSO	36.3 %	0.2	0.7	0.2	53.2 %	46.8 %
BGO	16.1 %	0.2	0.8	0.2	30.9 %	91.9 %

B. Manufactured PHC structures

The simulations provide data for manufacturing PHCs. Five PHC geometries were selected for the initial tests, given in Table. III. The first four are from the optimization simulations, and the last is inspired by literature [10]. These specific geometries were selected to help validate the modeling efforts and experimentally explore the impact of the Gap between the PHCs on the light transmission. The spacing between the features determines the required manufacturing resolution.

TABLE III
 PHC GEOMETRICAL PARAMETERS FOR FABRICATION

	Gap (μm)	PHC x (μm)	PHC z (μm)	Transmission	Improvement
1	0.22	1	0.3	59.0 %	62.8 %
2	0.5	1	0.3	48.3 %	33.2 %
3	0.7	1	0.3	45.6 %	25.9 %
4	0.8	1	0.3	43.6 %	20.2 %
5	1	1	0.3	Literature Inspired [10]	

Fig. 12 illustrates the efforts to baseline and optimize the electron beam writing behavior on our prepared LYSO substrates. Fig. 12 (A) is a digital image showing 60 different permutations of varied processing parameters patterned onto the surface of one crystal to assess the optimal write conditions. The SEM micrographs are increasingly magnified in Fig. 12 (B-D) to look at the various patterns deposited and subsequently etched with plasma etching.

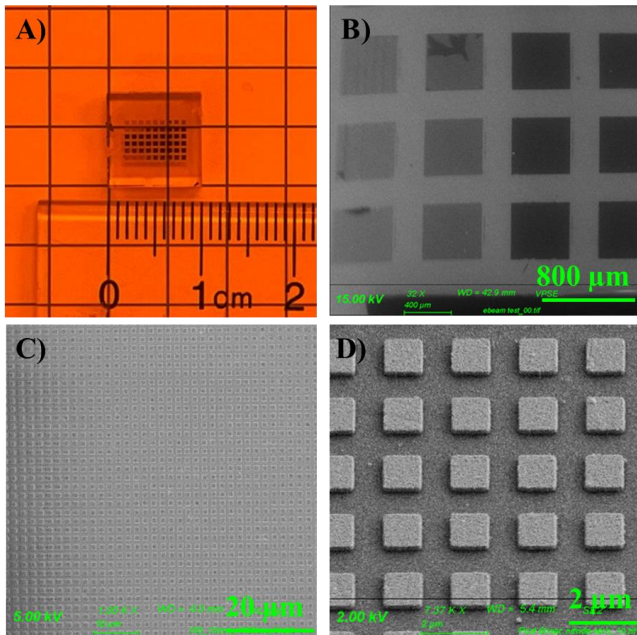


Fig. 12. E-Beam Lithography process optimization on A) a $10 \times 10 \times 3 \text{ mm}^3$ LYSO substrate, and increasing magnification of SEM micrographs B, C, & D) to observe the patterning.

The key exercise was to establish our optimal exposure energy and dose with respect to our pattern's density, resist material, resist thickness, and conductivity behavior of our resist-coated gold on silicon nitride. These variables must be optimized to achieve the pattern fidelity and resolution of interest. The optimal electron beam lithography processing window is highlighted in Fig. 13. The pillar arrays were etched and developed with good resolution. However, initial observations revealed that the lateral accuracy was off by $\sim 15\%$. This will be corrected in the subsequent manufacturing. Furthermore, our target PHC z- thickness was 300 nm, but our etching rate will also need to be adjusted as our total milled depth was only $\sim 130 \text{ nm}$, as observed in Fig. 13(Top right).

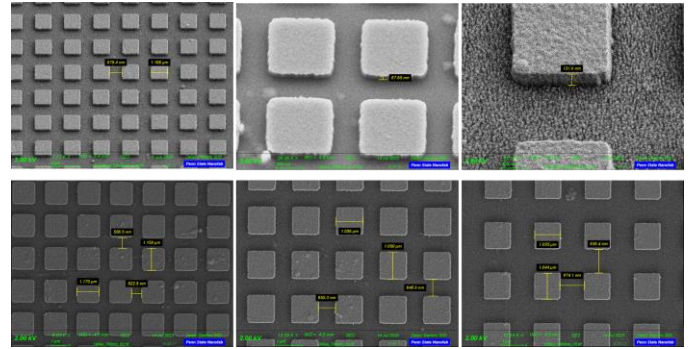


Fig. 13. Various SEM micrographs of optimal milled structures from the preliminary electron beam lithography trials.

These minor adjustments will be implemented for the final manufacturing process to prepare the five samples listed in Table. III.

IV. CONCLUSIONS

This project is a collaborative effort to simulate, manufacture and test the enhancement of light output from inorganic scintillators using PHCs. The simulations are done for a LYSO and a BGO scintillator to optimize the 2D block structure PHC geometry for Si_3N_4 . Optimized PHC geometries show an improvement in light transmission of 46.8% for LYSO and 91.9% for BGO. For LYSO, further simulations were done to improve light transmission by 62.8%. These optimized geometries are then manufactured in the lab.

The manufacturing process has been discussed in detail. We did 60 permutations of varied processing parameters to understand the optimal write conditions. We obtained a high-resolution, low-defect PHC geometry using electron beam lithography. Radiation measurements are also done between manufacturing steps to account for the optical defects produced by each step. This process allowed us to identify that DC magnetron sputtering damaged our crystal's optical properties. This was resolved using RF sputtering to deposit Si_3N_4 thin films, a primary manufacturing step.

The future work will characterize these PHC geometries with radiation measurements as outlined in the paper. We will also stimulate and validate other PHC shapes and structures for different scintillator materials.

ACKNOWLEDGMENT

This research is sponsored by the Defense Threat Reduction Agency (DTRA) as part of the Interaction of Ionizing Radiation with Matter University Research Alliance (IIRM-URA) under contract number HDTRA1-20-2-0002

REFERENCES

1. C. Dujardin *et al.*, "Needs, Trends, and Advances in Inorganic Scintillators," in *IEEE Transactions on Nuclear Science*, vol. 65, no. 8, pp. 1977-1997, Aug. 2018, doi: 10.1109/TNS.2018.2840160.
2. M. Salomoni, R. Pots, E. Auffray, and P. Lecoq, "Enhancing light extraction of inorganic scintillators using photonic crystals," *Crystals*, 8(2), 78, 2018, <https://doi.org/10.3390/cryst8020078>
3. J.D. Joannopoulos, S.G. Johnson, J.N. Winn, and R.D. Meade, *Photonic Crystals: Modeling the flow of light* 2nd ed. Princeton University Press, 2008, pp 2, 156-161.
4. C. Wiesmann, K. Bergenek, N. Linder, and U.T. Schwarz. (2009), Photonic crystal LEDs – designing light extraction. *Laser & Photon. Rev.*, 3: 262-286. <https://doi.org/10.1002/lpor.200810053>
5. M. Kronberger, E. Auffray and P. R. Lecoq, "Improving light extraction from heavy inorganic scintillators by photonic crystals," in *IEEE Transactions on Nuclear Science*, vol. 57, no. 5, pp. 2475-2482, Oct. 2010, doi: 10.1109/TNS.2010.2063438.
6. A. Knapitsch, E. Auffray, C.W. Fabjan, J. Leclercq, P. Lecoq, X. Letartre, C. Seassal, "Photonic crystals: a novel approach to enhance the light output of scintillation based detectors," *Nuclear Instruments and Methods in Physics Research Section A: Accelerators, Spectrometers, Detectors and Associated Equipment*, Volume 628, Issue 1,2011, Pages 385-388, ISSN 0168-9002, <https://doi.org/10.1016/j.nima.2010.07.007>
7. J. Allison *et al.*, "Recent developments in Geant4," Nuclear Instruments & Methods in Physics Research. Section A, Accelerators, Spectrometers, Detectors and Associated Equipment, vol. 835, (C), pp. 186-225, 2016.
8. Optifdtd overview (Jun 2020). <https://optiwave.com/optifdtd-overview/>
9. S. R. Surani, P. E. Albert, F. Logoglu, D.E. Wolfe, and M. Flaska, "Light-extraction chracterization and optimization for 2-D photonic crystals," in *Proc. INMM & ESARDA joint annual meeting*, Vienna, Austria, 2023
10. A. Knapitsch *et al.*, "Results of Photonic Crystal Enhanced Light Extraction on Heavy Inorganic Scintillators," in *IEEE Transactions on Nuclear Science*, vol. 59, no. 5, pp. 2334-2339, Oct. 2012, doi: 10.1109/TNS.2012.2184556.